Severe Pneumococcal Pneumonia Causes Acute Cardiac Toxicity and Subsequent Cardiac Remodeling

Reyes, Luis F.; Restrepo, Marcos I.; Hinojosa, Cecilia A.; Soni, Nilam J.; Anzueto, Antonio; Babu, Bettina L.; Gonzalez-Juarbe, Norberto; Rodriguez, Alejandro H.; Jimenez, Alejandro; Chalmers, James D.; Aliberti, Stefano; Sibila, Oriol; Winter, Vicki T.; Coalson, Jacqueline J.; Giavedoni, Luis D.; Dela Cruz, Charles S.; Waterer, Grant W.; Witzenrath, Martin; Suttorp, Norbert; Dube, Peter H.; Orihuela, Carlos J.

Published in:
American Journal of Respiratory and Critical Care Medicine

DOI:
10.1164/rccm.201701-0104OC

Publication date:
2017

Document Version
Accepted author manuscript

AJRCCM Articles in Press. Published on 14-June-2017 as 10.1164/rccm.201701-0104OC

TITLE: Severe Pneumococcal Pneumonia Causes Acute Cardiac Toxicity and Subsequent Cardiac Remodeling

AUTHORS: Luis F. Reyes[1, 2#], Marcos I. Restrepo[1, 2#], Cecilia A. Hinojosa[1, 2], Nilam J. Soni[1, 2], Antonio Anzueto[1,2], Bettina L. Babu[1, 2], Norberto Gonzalez-Juarbe[3], Alejandro H. Rodriguez[4], Alejandro Jimenez[5], James D. Chalmers[6], Stefano Aliberti[7], Oriol Sibila[8], Vicki T. Winter[9], Jacqueline J. Coalson[9], Luis D. Giavedoni[10], Charles S. Dela Cruz[11], Grant W. Waterer[12], Martin Witzenrath[13], Norbert Suttorp[13], Peter H. Dube[14] and Carlos J. Orihuela[3].

AFFILIATIONS: [1]Division of Pulmonary Diseases & Critical Care Medicine, The University of Texas Health Science Center at San Antonio, San Antonio, TX; [2]Division of Pulmonary Diseases & Critical Care Medicine, South Texas Veterans Health Care System, San Antonio, TX, USA; [3]Department of Microbiology, The University of Alabama at Birmingham, Birmingham, AL, USA; [4]Hospital Universitari Joan XXIII, Critical Care Medicine, Rovira & Virgili University and CIBERes (Biomedical Research Network of Respiratory disease), Tarragona, Spain; [5]Cardiovascular Medicine, Heart & Vascular Institute, Cleveland Clinic, Abu Dhabi, UAE; [6]School of Medicine, University of Dundee, Dundee, UK, [7]Department of Pathophysiology and Transplantation, University of Milan, Cardio-thoracic unit and Adult Cystic Fibrosis Centre, Fondazione IRCCS Ca' Granda Ospedale Maggiore Policlinico, Milan, Italy; [8]Servei de Pneumologia, Departament de Medicina, Hospital Santa Creu i Sant Pau, Universitat Autònoma de Barcelona, Spain; [9]Department of Pathology, The University of Texas Health Science Center at San Antonio, San Antonio, TX, USA; [10]Texas Biomedical Research Institute, San Antonio, TX ; [11]Division of Pulmonary and Critical Care Medicine, Yale University, New

Haven, Connecticut, USA; [12]Royal Perth Hospital Unit, University of Western Australia, Perth, Australia; [13]Department of Infectious Diseases and Pulmonary Medicine, Charité-Universitätsmedizin Berlin and SFB-TR84 "Innate Immunity of the Lung", Berlin, Germany; [14]Department of Immunology and Microbiology, The University of Texas Health Science Center at San Antonio, San Antonio, TX, USA;
#Co-first authors.

CORRESPONDING AUTHOR: Marcos I. Restrepo, MD, MSc; South Texas Veterans Health Care System ALMD - 7400 Merton Minter Boulevard - San Antonio Texas, 78229; Phone: (210)-617-5300 ext. 15413 - Fax: (210) 567-4423; Email: restrepom@uthscsa.edu

AUTHOR CONTRIBUTIONS: LFR, MIR, CAH, BLB, NJS, NGJ and CJO wrote and edited the manuscript. LFR, MIR and CJO designed the experiments. LFR, MIR, BLB and CAH executed the experiments. LFR, MIR, CAH, NJS, AHR, AJ, JDC, VTW, JJC, NGJ, LDG, AA, PHD and CJO provided experimental technical support. LFR, MIR, CAH, NJS, AA, BLB, NGJ, AHR, AJ, JDC, SA, OS, VTW, JJC, LDG, CDC, GWW, MW, NS, PHD and CJO contributed intellectually.

FINANCIAL SUPPORT: MIR's time is partially protected by Award Number K23HL096054 from the National Heart, Lung, and Blood Institute. CJO receives support from NIH grant AI114800 and American Heart Association 16GRNT30230007. This investigation used resources that were supported by the Southwest National Primate Research Center grant P51 OD011133 from the Office of Research Infrastructure Programs, NIH. The content is solely the

AJRCCM Articles in Press. Published on 14-June-2017 as 10.1164/rccm.201701-0104OC

responsibility of the authors and does not necessarily represent the official views of the National Heart, Lung, And Blood Institute or the National Institutes of Health nor the Department of Veterans Affairs.

RUNNING TITLE: Cardiotoxicity in baboons during pneumococcal pneumonia

DESCRIPTOR NUMBER: 10.12 (Pneumonia: Bacterial Infections)

TOTAL WORD COUNT: 3,500 (Limit 3,500)

ABSTRACT WORD COUNT: **247** (Limit 250)

AT A GLANCE COMMENTARY

Scientific Knowledge on the Subject: *Streptococcus pneumoniae* is the most frequently isolated bacterial pathogen in patients with community-acquired pneumonia (CAP). As result of highly complex host-pathogen interactions, patients with pneumococcal pneumonia are at increased risk of developing cardiovascular complications during and after CAP, including heart failure, arrhythmias, strokes, and acute coronary syndromes. Recent studies in mice revealed that *S. pneumoniae* is capable of invading the heart and causing direct cardiac damage during invasive pneumococcal disease. Yet, murine pneumococcal pneumonia is poorly representative of human disease and whether cardiac invasion occurs during severe pneumonia in humans is unknown. Our aim was to determine if pneumococcus 1) invades the myocardium, 2) induces cardiomyocyte death, and 3) elicits cardiovascular complications during pneumococcal pneumonia, using a validated non-human primate model that closely resembles pneumococcal disease in humans.

What This Study Adds to the Field: This study presents novel evidence that *S. pneumoniae* can invade the heart during severe pneumonia and induces cardiomyocyte death via direct cytotoxic effects. These findings could potentially explain the development of short- and long-term cardiac complications associated with CAP due to acute cardiomyocyte injury and induction of scar formation in the hearts of convalescent non-human primates.

This article has an online data supplement, which is accessible from this issue's table of content online at www.atsjournals.org

AJRCCM Articles in Press. Published on 14-June-2017 as 10.1164/rccm.201701-0104OC

ABSTRACT

Rationale: Up to one-third of the patients hospitalized with pneumococcal pneumonia experience major adverse cardiac events (MACE) during or after pneumonia. In mice, *Streptococcus pneumoniae* can invade the myocardium, induce cardiomyocyte death, and disrupt cardiac function following bacteremia, but it is unknown whether the same occurs in humans with severe pneumonia.

Objective: We sought to determine whether *S. pneumoniae* can 1) translocate the heart, 2) induce cardiomyocyte death, 3) cause MACE, and 4) induce cardiac scar formation post-antibiotic treatment during severe pneumonia using a non-human primates (NHP) model.

Methods: We examined cardiac tissue from six adult NHP with severe pneumococcal pneumonia and three uninfected controls. Three animals were rescued with antibiotics (convalescent animals). Electrocardiogram (ECG), echocardiogram, and serum biomarkers of cardiac damage were performed (troponin-T, NT-proBNP and H-FABP). Histologic examination included hematoxylin & eosin (H&E) staining, immunofluorescence, immunohistochemistry, picosirus red staining and transmission electron microscopy (TEM). Immunoblots were used to assess the underlying mechanisms.

Measurements and Main Results: Non-specific ischemic alterations were detected by ECG and echocardiogram. Serum levels of troponin-T and H-FABP levels were increased ($p=<0.05$) after pneumococcal infection in both, acutely-ill and convalescent NHP. *S. pneumoniae* was detected in the myocardium of all NHP with acute severe pneumonia. Necroptosis and apoptosis were detected in myocardium of both, acutely-ill and convalescent NHP. Evidence of cardiac scar formation was observed only in convalescent animals by TEM and picosirus red staining.

Conclusions: *S. pneumoniae* invades the myocardium, induces cardiac injury with necroptosis and apoptosis, followed by cardiac scarring after antibiotic therapy, in a non-human primate model of severe pneumonia.

ABSTRACT WORD COUNT: 250 (Limit 250)

Key words (3-5): Pneumococcal pneumonia, *Streptococcus pneumoniae*, cardiovascular complications, community-acquired pneumonia

AJRCCM Articles in Press. Published on 14-June-2017 as 10.1164/rccm.201701-0104OC

INTRODUCTION

Lower respiratory tract infections cost the healthcare system more than 10 billion dollars annually in the United States (1, 2). Community-acquired pneumonia (CAP) and influenza infections together are the fourth most prevalent cause of death worldwide (3). The morbidity, mortality, and costs associated with CAP have remained unchanged in recent decades, despite availability of antibiotic treatments and preventive strategies with immunizations (4, 5). Approximately 30% of patients hospitalized with CAP experience major adverse cardiac events (MACE) during hospitalization up to ten years post-infection (6-9). Importantly, patients with pneumonia and MACE have double the hospital mortality compared to those with pneumonia alone (6, 10). MACE in CAP patients include new onset or worsening heart failure, arrhythmias, stroke, and acute coronary syndromes (9). Risk factors for a MACE during CAP include infection due to *S. pneumoniae*, older age, severe CAP, hyperlipidemia, obesity, and arterial hypertension (6, 8, 11, 12). The pathophysiology of MACE during CAP has been attributed to the complex host-pathogen interactions, but the exact mechanisms are not well understood (9, 13).

Streptococcus pneumoniae (pneumococcus) is the most frequent bacterial pathogen in patients with CAP (14, 15). Pneumococcal pneumonia has been identified as an independent risk factor for the development of MACE during CAP (6, 8, 11, 12, 16). Pneumococcal pneumonia can result in cardiovascular complications in 10-30% of patients, affecting mainly those with existing cardiovascular diseases (11, 12). Recently, our research group (17, 18) and others (19-21) have described that the pneumococcus and its virulence factors (e.g., pneumolysin, bacterial cell wall, etc.) have direct detrimental effects on the cardiac function of rodents with invasive pneumococcal disease (IPD). We have demonstrated that pneumococcus can invade the heart,

and cause small, bacteria-filled lesions within the myocardium (17, 18). These myocardial lesions disrupt cardiac contractility, induce cardiomyocyte death, and subsequently cause *de novo* collagen deposition in mice rescued with antibiotics (convalescent mice) (17, 22). Moreover, we have shown that *S. pneumoniae* is capable of inducing necroptosis, a highly proinflammatory programmed cell-death pathway, in lung macrophages during pneumonia (23). Pertinent to the present study, necroptosis has been recognized as a key cell death pathway in cardiomyocytes during ischemia-reperfusion injury and acute coronary syndromes (24-26).

Despite epidemiological studies demonstrating pneumococcal infection is an independent risk factor for MACE (6-8, 11, 12), it is unknown whether *S. pneumoniae* can generate direct cardiac cytotoxicity (e.g., cell-death), heart failure, clinically relevant arrhythmias, or acute coronary syndromes (i.e., MACE) in humans with severe pneumococcal pneumonia (11, 12, 16, 27). Additionally, the potential underlying mechanisms of MACE during pneumococcal pneumonia have been described in rodent models, but it is speculative to extrapolate these findings to humans. To address this knowledge gap, we used a validated non-human primate model of severe pneumococcal pneumonia that closely mimics human disease (28) to explore the mechanisms of pneumococcal cytotoxicity on cardiomyocytes. Potential translation of these findings to humans includes identification of potential therapeutic targets to prevent MACE, and ultimately, improvement in clinical outcomes of patients with CAP.

MATERIALS AND METHODS

Animal studies were performed at the Texas Biomedical Research Institute (TBRI) in San Antonio, Texas. This animal protocol along with all animal experiments were reviewed and approved by the Institutional Animal Care and Use Committee (IACUC Number 1443PC6) at

AJRCCM Articles in Press. Published on 14-June-2017 as 10.1164/rccm.201701-0104OC

the TBRI.

Study Design

A full description of the NHP model of severe pneumococcal pneumonia has been previously published (28). Briefly, six (four males) healthy adult baboons (*Papio cynocephalus*) were bronchoscopically challenged with 10^9 colony-forming units (CFU) of *S. pneumoniae* serotype 4 (strain TIGR4 (29)). Collection of blood for serum biomarkers and bacterial load estimation, acquisition of a 12-lead electrocardiogram (ECG), transthoracic echocardiogram, and bronchoalveolar lavage (BAL) were performed before the infection and at the end of the experiment prior to euthanasia (28). Continuous 24-hour temperature, heart rate, and 3-lead ECG were recorded throughout the experiment via a surgically implanted tether. At the end of the experiment, the hearts were harvested and prepared for tissue experiments. Three NHP were treated with intravenous ampicillin (80mg/kg/day) for 7 days (i.e., convalescent group) (28). All ECGs were read by an expert electrophysiologist (AJR) who was blinded to the experiment results. The study design is summarized in the Fig. A of the online supplement. Finally, major adverse cardiac events (MACE) were defined as heart failure, arrhythmias or myocardial infarctions.

Study groups

The cohort was divided in two groups to mimic the pre-antibiotic era and modern era of pneumonia patients (28). For the pre-antibiotic era group, we did not treat three NHP with antibiotics, and they were called the *acute pneumonia* and euthanized per protocol, 4-6 days post-infection. In contrast, the modern era of pneumonia group, three NHP were rescued with antibiotic treatment, and they were called the *convalescent pneumonia* and euthanized per protocol, 9-14 days post infection (28). The end of experiment refers to the moment before

euthanasia, that varies for each animal according with the study groups descried above (28). Heart tissues of three age- and gender-matched uninfected NHP served as controls (Fig. A of the online supplement).

Transthoracic Echocardiogram Evaluation

A standard 5-view focused cardiac ultrasound exam was performed using a portable ultrasound machine (General Electric Logiq-E Vet) equipped with microconvex (GE model 8C-RS, 4.0-10.0 MHz) and phased-array (GE model 3S-RS,1.7-4.0 MHz) transducers. Parasternal long- and short-axis, apical and subcostal 4-chambers, and subcostal inferior vena cava (IVC) views were obtained to assess the left (LV) and right (RV) ventricular size and function, cardiac valves, pericardium, and IVC size and collapsibility.

Serum Cardiac Biomarkers

Serum levels of ultra-sensitive Troponin T (Life Diagnostics), Heart Fatty Acid Binding Protein (H-FABP, Kamiya Biomedical) and N-terminal pro-brain natriuretic peptide (NT-proBNP, Neo Scientific) were measured by enzyme-linked immunosorbent assay (ELISA) in serum samples pre-infection and at the end of the experiment. Cytokine and chemokine analyses were performed using a validated luminex multiplex assay for NHP (30).

Tissue Staining and Microscopy

Immunofluorescence (IF) and immunohistochemistry (IHC) were performed in paraffin embedded tissues as previously described (18). Primary antibodies used in this study included those against serotype 4 capsular polysaccharide antibody (Staten's Serum Institut); pneumolysin (Ply, Santa Cruz Biotechnology), transforming growth factor (TGF)-β (Bio-Rad Laboratories), pSMAD3, mixed lineage kinase domain like pseudokinase (MLKL), p-MLKL, Caspase 3 (Cell Signaling Technology), receptor-interacting protein kinase 3 (RIP3) (Abcam), and hypoxia

AJRCCM Articles in Press. Published on 14-June-2017 as 10.1164/rccm.201701-0104OC

inducible factor 1 (HIF1)-α (Bethyl Laboratories). The secondary antibody used was fluorescein isothiocyanate (FITC) labeled goat anti-rabbit antibody (Jackson Immuno Research). Picosirus red (Electron Microscopy Sciences), and H&E stained heart sections were scanned with the Aperio Scanscope XT (Aperio). IF and IHC images were captured with an Olympus AX70 microscope. Transmission electron microscopy (TEM) images were obtained with a JEOL JEM1230 transmission electron microscope (Peabody).

Immunoblots

Hearts were homogenized and processed as previously described (23) with protease (Sigma) and phosphatase (Thermo Scientific) inhibitors.

Statistical Analysis

All data are presented as medians with interquartile ranges (IQR), or means with standard deviations (SD) as appropriate. Pared non-parametric Wilcoxon signed rank test or two-tailed Student's *t*-test were used to compare data at different time points. All statistical calculations were performed using Prism 5 software (GraphPad). Two tails p-values <0.05 were considered statistically significant.

RESULTS

Six NHP with a median age of 11 (IQR, 10-19) years old, which corresponds to middle-aged to elderly humans were included in the study. Details about each NHP, and an overview of the experiments to develop the severe pneumococcal pneumonia model were previously described (28). Demographics and pneumonia severity are presented in Table A of the online supplement.

Non-invasive Cardiac Evaluation

Electrocardiography Evaluation

During baseline evaluation, all animals were in sinus rhythm with normal PR, QT, and ST intervals (Table 1, Fig. 1A); P, T and QRS waves resembled their normal morphology in humans (Fig. 1A). At the end of the experiment, immediately prior to euthanasia, ECG evaluation showed that all 6 NHP had developed sinus tachycardia, diffuse repolarization abnormalities represented by diffuse ST segment changes, T waves flattening, and prolongation of the corrected QT interval (QTc) (Figs. 1B-E, Table 1). Table 2 presents the individual interpretations of the 12-lead ECGs at baseline and at the end of the experiment. No other significant alterations were detected in the ECG tracings, even after the cohort was stratified by acute or convalescent pneumonia (Table B of the online supplement).

Echocardiogram Findings

A qualitative focused cardiac ultrasound (FCU) examination was conducted at baseline and at the end of the experiment. Findings are summarized in Table C in the online supplement**.** Prior to infection, all 6 NHP had a normal FCU exam. NHP with acute pneumonia demonstrated hyperdynamic LV function, moderate tricuspid regurgitation, small pericardial effusions, and collapsed IVC's (central venous pressure (CVP) <5). NHP with convalescent pneumonia developed increased LV relative wall thickness and some associated wall motion abnormalities (hypokinesis).

Serum Biomarkers

Troponin T and H-FABP serum levels were elevated at the end of experiment in all NHP compared to baseline levels (median [IQR]; 0.005ng/mL [0.000, 0.025] vs 0.044ng/mL [0.036, 0.057], p=0.002; 150.8ng/mL [33.25, 281.5] vs 916.9ng/mL [595.8, 1323], p=0.002,

AJRCCM Articles in Press. Published on 14-June-2017 as 10.1164/rccm.201701-0104OC

respectively) (Figs. 2A and C). When we stratified the cohort by acute or convalescent pneumonia (i.e., with and without antibiotic treatment), Troponin T and H-FABP remained higher at the end of the experiment in both cohorts, but Troponin T concentration was not statistically significant higher than baseline (Figs. 2B and D). In contrast, serum NT-proBNP serum levels did not change significantly at the end of the experiment (194.2pg/mL [22.21, 815.1] vs 141.9pg/mL [39.8, 565.5], p=0.9) (Figs. 2E and F).

Invasive cardiac evaluation

Detection of Streptococcus pneumoniae

We performed immunofluorescent staining of the different parts of the heart in all animals and confirmed the invasion of *S. pneumoniae* in the myocardium (Fig. 3A and B). In NHP with acute pneumonia, we observed clusters of pneumococci suggesting that the bacteria were capable of replicating within the tissue. In contrast, in NHP with convalescent pneumonia, only a few punctate points were observed, representing *S. pneumoniae* capsule debris (Fig. 3C). Quantification of bacteria in heart homogenates confirmed that *S. pneumoniae* were present in NHP with acute pneumonia, and none were detected in those with convalescent pneumonia nor in uninfected controls (Fig. B of the online supplement).

Histopathological Findings

Tissue sections of the right or left ventricle and the interventricular septum showed similar lesions of a focal cardiac injury primarily in perivascular sites of varying extent and severity by H&E staining (Fig. C of the online supplement). Affected cardiac myocytes were enlarged with a striking increase in eosinophilic staining and were well demarcated from adjacent cardiac tissue (Figs. 4A-C). The damage of left ventricles and septum varied in size and

infiltration (Fig. C of the online supplement). Varying degenerative and/or necrotic lesions were observed in the left ventricle and interventricular septum (Figs. 4A-C). All animals had mild to severe myocyte fatty change and vacuolization, focal contraction bands, interstitial edema, focal myocytolysis, and scattered inflammatory cells (Figs. 4A and B). We observed scattered myocytolysis in several myocytes (Figs 4A and B), but prominent nuclear pyknosis with extensive myocytolysis were apparent in several myocytes (Fig. 4C). Two NHP exhibited additional necrotic lesions defined by nuclear karyolysis and fragmentation, although one site had some clumped bacteria (Fig. 4C).

Using transmission electron microscopy (TEM), we observed that infected NHP consistently developed areas of vacuolization with focal contraction bands, and interstitial edema in the left ventricle and septum (Fig. 4E and F). Additionally, we identified several areas with focal myocytolysis and nuclear pyknosis that corresponded with extensive mitochondrial damage characterized by swollen and electron lucent matrices (Fig. 4G). Moreover, the mitochondrial cristae were degraded and disorganized, and with decreased density. All these changes were evident in both the acute and convalescent pneumonia groups (Fig. 4E-G).

Cardiac Inflammatory Response

We observed high concentrations of cytokines and chemokines, including IL-6, TNF-α, IL-8, IL-1β, IL-1Rα, and MIP-1α, in homogenized hearts (left ventricle and interventricular septum) of all NHP with acute pneumonia (Fig. 5). All three NHP with convalescent pneumonia had lower heart concentrations of cytokines and chemokines levels compared to NHP with acute pneumonia (Fig. 5A-F). Significantly higher concentrations of IL-6, TNF-α, and IL-1β were seen in the left ventricle and interventricular septum of infected NHP vs. uninfected controls (Fig. 5B,

AJRCCM Articles in Press. Published on 14-June-2017 as 10.1164/rccm.201701-0104OC

D and E). IL-8 levels were higher in the interventricular septum (Fig. 5C) of NHP with convalescent pneumonia vs. uninfected controls.

Cardiomyocyte Death

To test the role of necroptosis in cardiomyocyte death, we stained for RIP3 and pMLKL (necroptosis effector) in heart tissues from infected NHP with acute and convalescent pneumonia and uninfected controls using IHC staining (Fig. 6A). An increased signal of both RIP3 and pMLKL was seen in stained tissues, suggesting necroptosis was taking place throughout the myocardium. Increased levels of both RIP3 and pMLKL were confirmed by immunoblot (Fig. 6B**).** Additional staining of cardiac tissues with CardioTAC suggested apoptotic cells in the myocardium (Fig. D of the Online Supplement). Briefly, CardioTAC labels DNA ends using terminal deoxynucleotidyl transferase. In addition, consistent with the presence of apoptotic cells in the myocardium, we observed an increase of apoptosis effector caspase-3 mainly in NHP with acute pneumonia (Fig. D of the Online Supplement). Collectively these results suggest that *S. pneumoniae* induces programmed death pathways after its invasion of the myocardium.

Cardiac fibrosis

TGF-β in the heart stimulates myofibroblasts to produce collagen to replace dead cardiomyocytes (31, 32). After *S. pneumoniae* had induced necroptosis in the heart, *de novo* collagen deposition was detected in the left ventricle and septum evident by picosirus red staining (Fig. 7A) and TEM (Fig. 7B). Collagen deposition was seen 9-14 days post-infection in convalescent animals. Additionally, using immunoblot, we identified increased expression of pSMAD3 which stimulates collagen production in cardiac myofibroblasts (33).

Finally, to confirm that cardiac injury and collagen deposition were secondary to *S. pneumoniae* invasion, we explored the HIF1-α pathway that is activated by hypoxia (34).

Immunoblots in homogenized hearts of NHP confirmed the HIF1-α pathway was downregulated in both acute and convalescent pneumonia groups (Fig. E of the Online Supplement).

DISCUSSION

The results of our study provide novel evidence that, similar to humans, NHP with severe pneumococcal pneumonia develop signs of cardiac injury, including diffuse repolarization abnormalities, hyperdynamic left ventricle function, and mild elevations of serum biomarkers (i.e., troponin T and H-FABP). Microscopic examination of heart tissues revealed that pneumococcus is capable of translocating into the myocardium and induce cardiomyocytes by necroptosis and apoptosis. Moreover, we confirmed that heart invasion by *S. pneumoniae* causes severe cardiac injury and local proinflammatory responses independent of antibiotic treatment. We provided evidence that NHP with convalescent pneumonia develop interstitial collagen deposition (i.e., scar formation) secondary to the TGF-β pathway activation. Our findings are novel as they provide translational data highlighting the etiologic role of *S. pneumoniae* in causing MACE in patients with pneumonia. Further, collagen deposition in the myocardium may explain the increased long-term risk of MACE after an acute episode of pneumococcal pneumonia.

Up to 36% of patients hospitalized with CAP develop severe disease that requires admission to the intensive care unit (ICU) (35, 36). Due to the severe inflammatory response and mitochondrial dysfunction during severe pneumonia, at least 30% of patients develop left ventricular dilatation with reduced ejection fraction that usually takes 7-10 days to recover (i.e., sepsis-induced cardiomyopathy) (37, 38). In addition, Corrales-Medina *et al* showed recently in a cohort study that 10-30% of adults (without clinical history of cardiac disease) admitted for

AJRCCM Articles in Press. Published on 14-June-2017 as 10.1164/rccm.201701-0104OC

CAP, developed clinically relevant heart failure, arrhythmias, or acute coronary syndromes, up to 10 years after hospitalization (6-8). More commonly, up to 59% of patients admitted with sepsis develop a cardiac phenomenon called demand ischemia (i.e., mild troponin elevation and repolarization abnormalities in absence of myocardial infarction or coronary disease), rather than sepsis-induced cardiomyopathy or MACE (39-41). In our study, we found that all six previously healthy NHP with pneumococcal pneumonia, developed nonspecific cardiac changes that cannot be categorized as MACE but are consistent with what clinicians call demand ischemia. In contrast to humans, we were able to perform a detailed *ex-vivo* examination of the NHP hearts, which revealed that *S. pneumoniae* can invade the heart and induce severe cardiac injury by killing cardiomyocytes through necroptosis and apoptosis.

S. pneumoniae and its virulence factors (e.g., pneumolysin, cell wall, etc.) are cytotoxic and capable of inducing inflammation in cardiomyocytes (17, 19, 20). Recently, our research group described the novel observation that the pneumococcus is capable of invading the myocardium and forming non-purulent, bacteria-filled, microscopic lesions that were associated with cardiomyocyte death (apoptosis) and electrocardiographic abnormalities in mice with IPD (22). In our experiments with severe pneumococcal pneumonia in NHP, we proved that the pneumococcus is capable of invading the bloodstream and translocating the myocardium. In contrast to mice, the hearts of NHP showed *S. pneumoniae* in clusters, representing active replication, that did not form microlesions as previously described in mice (18). This difference may be explained by the high bacterial load and longer infection times required to develop mature microlesions. Gilley *et al (18)* recently described how cardiac invasion by pneumococcus occurs as soon as 12 hours after infection, but microlesion formation was bacterial load and time-dependent. Although similar findings have been seen in an IPD model

that is not representative of pneumococcal pneumonia in humans, we used an NHP model of severe pneumonia that closely mimics the development and pathogenesis of human disease in which all the animals develop low-grade bacteremia for a short period (28).

Cardiomyocytes have been shown to die by apoptosis or necroptosis during injury or disease (24-26). Apoptosis is an immunoquiescent form of cell death that requires the activity of cysteine proteases known as caspases (42). It has been shown that mice lacking the death receptor FAS or mice treated with chemical inhibitors of caspases experience reduced heart infarct sizes and less apoptotic positive cells after ischemic and reperfusion injuries (43). Opposite of apoptosis, necroptosis, or programmed necrosis, causes severe inflammation and tissue damage during disease (44). Necroptosis is modulated by activation of receptor-interacting serine/threonine-protein kinase (RIP) 1, RIP3, and the effector molecule MLKL (25, 45). Recently, Yin B *et al* showed that a non-specific inhibitor of RIP1, necrostatin-1, could reduce infarct sizes after major ischemic or reperfusion injuries (46). Using an NHP model, we showed that cardiomyocytes undergo RIP1-RIP3-MLKL dependent necroptosis and necroptosis inhibition with a selective drug has been shown to be protective against *S. pneumoniae* induced cardiac damage as reported by Gonzalez-Juarbe [Companion manuscript]. This finding is significant because killing cardiomyocytes and inducing a proinflammatory response may contribute to the generation of MACE during pneumococcal pneumonia.

Antibiotics have been shown to drastically reduce mortality due to pneumonia and other infectious diseases and are the cornerstone of CAP treatment (5). Thus, to mimic the disease evolution of CAP in humans, we treated NHP with ampicillin to explore whether antibiotic treatment could prevent the development of cardiac injury secondary to *S. pneumoniae* invasion. We revealed that antibiotic treatment did not protect NHP from the development of necroptosis

AJRCCM Articles in Press. Published on 14-June-2017 as 10.1164/rccm.201701-0104OC

or cardiac injury, and more important, NHP treated with antibiotics formed scars in the heart. These findings are consistent with our findings in mice rescued from IPD with antibiotics (17), and other experiments in mice with ischemia/reperfusion injury (31). This finding improves our understanding of MACE and long-term mortality of CAP patients. As described by Souders CA *et al,* once cardiomyocytes die, heart tissue is replaced with myofibroblasts that produce an extracellular matrix that is rich in collagen and leads to scar formation (47). Because *S. pneumoniae* is capable of inducing cardiac scar formation and cardiac scars are known to cause arrhythmias and heart failure, our findings might explain why MACE occur up to 10 years after the acute infection.

MACE are the result of a complex host-pathogen interaction between underlying co-morbidities, the infectious pathogen (9), systemic inflammation (48), endothelial dysfunction (49), relative prothrombotic state (9), increased cardiac oxygen demand, and low blood oxygen levels that place considerable stress on the heart (9). In this study, we have shown that pathogen-specific mechanisms of *S. pneumoniae* contribute to the development of cardiac damage during pneumococcal pneumonia that could lead to MACE.

Our study has some important limitations. First, the experimental design was limited to a two-week maximum duration, and findings should not be interpreted as long-term clinical outcomes after surviving CAP. Second, the clinical evaluation was limited in capabilities to continuously assess oxygenation or hemodynamic parameters that could associated with cardiac injury. However, at the end of the experiments, the NHP were not hypotensive to the level requiring vasopressor support. Third, we did not specifically exanimated coronary arteries to identify thrombus or signs of myocardial infarctions. But, we rollout the clinical diagnosis of myocardial infarction according with the current guidelines of the American Heart

Association(50). Finally, the sample size was limited to six NHP with pneumococcal pneumonia due to ethical considerations and high costs associated with the implantable continuous non-invasive cardiovascular monitoring systems and intensive veterinary medical care.

In summary, severe pneumococcal pneumonia led to development of cardiac injury due to direct pathogen invasion, induction of cell death (necroptosis and apoptosis), and subsequent cardiac scar formation after antibiotic treatment in a non-human primate model. Further research of strategies to mitigate the pathologic mechanisms underlying cardiac injury secondary to pneumococcal invasion are needed.

ACKNOWLEDGEMENTS

The authors thank Jessica Perry, Rene Escalona, Manuel Aguilar, and Johnny Saucedo at the Texas Biomedical Research Institute (San Antonio, TX) for their extraordinary efforts to make this project possible.

REFERENCES

1. Wunderink RG, Waterer GW. Community-acquired pneumonia. *The New England journal of medicine* 2014; 370: 1863.
2. Prina E, Ranzani OT, Torres A. Community-acquired pneumonia. *Lancet* 2015; 386: 1097-1108.
3. World Health Organization. The top 10 causes of death. Geneva. 2013.
4. Torres A, Sibila O, Ferrer M, Polverino E, Menendez R, Mensa J, Gabarrus A, Sellares J, Restrepo MI, Anzueto A, Niederman MS, Agusti C. Effect of corticosteroids on

AJRCCM Articles in Press. Published on 14-June-2017 as 10.1164/rccm.201701-0104OC

treatment failure among hospitalized patients with severe community-acquired pneumonia and high inflammatory response: a randomized clinical trial. *Jama* 2015; 313: 677-686.

5. Musher DM, Thorner AR. Community-acquired pneumonia. *The New England journal of medicine* 2014; 371: 1619-1628.
6. Corrales-Medina VF, Alvarez KN, Weissfeld LA, Angus DC, Chirinos JA, Chang CC, Newman A, Loehr L, Folsom AR, Elkind MS, Lyles MF, Kronmal RA, Yende S. Association between hospitalization for pneumonia and subsequent risk of cardiovascular disease. *Jama* 2015; 313: 264-274.
7. Corrales-Medina VF, Taljaard M, Yende S, Kronmal R, Dwivedi G, Newman AB, Elkind MS, Lyles MF, Chirinos JA. Intermediate and long-term risk of new-onset heart failure after hospitalization for pneumonia in elderly adults. *American heart journal* 2015; 170: 306-312.
8. Corrales-Medina VF, Taljaard M, Fine MJ, Dwivedi G, Perry JJ, Musher DM, Chirinos JA. Risk stratification for cardiac complications in patients hospitalized for community-acquired pneumonia. *Mayo Clinic proceedings* 2014; 89: 60-68.
9. Corrales-Medina VF, Musher DM, Shachkina S, Chirinos JA. Acute pneumonia and the cardiovascular system. *Lancet* 2013; 381: 496-505.
10. Corrales-Medina VF, Musher DM, Wells GA, Chirinos JA, Chen L, Fine MJ. Cardiac complications in patients with community-acquired pneumonia: incidence, timing, risk factors, and association with short-term mortality. *Circulation* 2012; 125: 773-781.

11. Viasus D, Garcia-Vidal C, Manresa F, Dorca J, Gudiol F, Carratala J. Risk stratification and prognosis of acute cardiac events in hospitalized adults with community-acquired pneumonia. *The Journal of infection* 2013; 66: 27-33.

12. Musher DM, Rueda AM, Kaka AS, Mapara SM. The association between pneumococcal pneumonia and acute cardiac events. *Clinical infectious diseases : an official publication of the Infectious Diseases Society of America* 2007; 45: 158-165.

13. Corrales-Medina VF, Suh KN, Rose G, Chirinos JA, Doucette S, Cameron DW, Fergusson DA. Cardiac complications in patients with community-acquired pneumonia: a systematic review and meta-analysis of observational studies. *PLoS medicine* 2011; 8: e1001048.

14. Jain S, Self WH, Wunderink RG, Fakhran S, Balk R, Bramley AM, Reed C, Grijalva CG, Anderson EJ, Courtney DM, Chappell JD, Qi C, Hart EM, Carroll F, Trabue C, Donnelly HK, Williams DJ, Zhu Y, Arnold SR, Ampofo K, Waterer GW, Levine M, Lindstrom S, Winchell JM, Katz JM, Erdman D, Schneider E, Hicks LA, McCullers JA, Pavia AT, Edwards KM, Finelli L, Team CES. Community-Acquired Pneumonia Requiring Hospitalization among U.S. Adults. *The New England journal of medicine* 2015; 373: 415-427.

15. Aliberti S, Reyes LF, Faverio P, Sotgiu G, Dore S, Rodriguez AH, Soni NJ, Restrepo MI, investigators G. Global initiative for meticillin-resistant Staphylococcus aureus pneumonia (GLIMP): an international, observational cohort study. *The Lancet Infectious diseases* 2016.

16. Rae N, Finch S, Chalmers JD. Cardiovascular disease as a complication of community-acquired pneumonia. *Current opinion in pulmonary medicine* 2016; 22: 212-218.

AJRCCM Articles in Press. Published on 14-June-2017 as 10.1164/rccm.201701-0104OC

17. Brown AO, Mann B, Gao G, Hankins JS, Humann J, Giardina J, Faverio P, Restrepo MI, Halade GV, Mortensen EM, Lindsey ML, Hanes M, Happel KI, Nelson S, Bagby GJ, Lorent JA, Cardinal P, Granados R, Esteban A, LeSaux CJ, Tuomanen EI, Orihuela CJ. Streptococcus pneumoniae translocates into the myocardium and forms unique microlesions that disrupt cardiac function. *PLoS pathogens* 2014; 10: e1004383.

18. Gilley RP, Gonzalez-Juarbe N, Shenoy AT, Reyes LF, Dube PH, Restrepo MI, Orihuela CJ. Infiltrated macrophages die of pneumolysin-mediated necroptosis following pneumococcal myocardial invasion. *Infection and immunity* 2016.

19. Alhamdi Y, Neill DR, Abrams ST, Malak HA, Yahya R, Barrett-Jolley R, Wang G, Kadioglu A, Toh CH. Circulating Pneumolysin Is a Potent Inducer of Cardiac Injury during Pneumococcal Infection. *PLoS pathogens* 2015; 11: e1004836.

20. Fillon S, Soulis K, Rajasekaran S, Benedict-Hamilton H, Radin JN, Orihuela CJ, El Kasmi KC, Murti G, Kaushal D, Gaber MW, Weber JR, Murray PJ, Tuomanen EI. Platelet-activating factor receptor and innate immunity: uptake of gram-positive bacterial cell wall into host cells and cell-specific pathophysiology. *Journal of immunology (Baltimore, Md : 1950)* 2006; 177: 6182-6191.

21. Feldman C, Anderson R. Recent advances in our understanding of Streptococcus pneumoniae infection. *F1000prime reports* 2014; 6: 82.

22. Brown AO, Millett ER, Quint JK, Orihuela CJ. Cardiotoxicity during invasive pneumococcal disease. *American journal of respiratory and critical care medicine* 2015; 191: 739-745.

23. Gonzalez-Juarbe N, Gilley RP, Hinojosa CA, Bradley KM, Kamei A, Gao G, Dube PH, Bergman MA, Orihuela CJ. Pore-Forming Toxins Induce Macrophage Necroptosis during Acute Bacterial Pneumonia. *PLoS pathogens* 2015; 11: e1005337.

24. Zhang T, Zhang Y, Cui M, Jin L, Wang Y, Lv F, Liu Y, Zheng W, Shang H, Zhang J, Zhang M, Wu H, Guo J, Zhang X, Hu X, Cao CM, Xiao RP. CaMKII is a RIP3 substrate mediating ischemia- and oxidative stress-induced myocardial necroptosis. *Nature medicine* 2016; 22: 175-182.

25. Linkermann A, Hackl MJ, Kunzendorf U, Walczak H, Krautwald S, Jevnikar AM. Necroptosis in immunity and ischemia-reperfusion injury. *American journal of transplantation : official journal of the American Society of Transplantation and the American Society of Transplant Surgeons* 2013; 13: 2797-2804.

26. Linkermann A, Brasen JH, Darding M, Jin MK, Sanz AB, Heller JO, De Zen F, Weinlich R, Ortiz A, Walczak H, Weinberg JM, Green DR, Kunzendorf U, Krautwald S. Two independent pathways of regulated necrosis mediate ischemia-reperfusion injury. *Proceedings of the National Academy of Sciences of the United States of America* 2013; 110: 12024-12029.

27. Restrepo MI, Reyes LF, Anzueto A. Complication of Community-Acquired Pneumonia (Including Cardiac Complications). *Seminars in respiratory and critical care medicine* 2016; 37: 897-904.

28. Reyes LF, Restrepo MI, Hinojosa CA, Soni NJ, Shenoy AT, Gilley RP, Gonzalez-Juarbe N, Noda JR, Winter VT, de la Garza MA, Shade RE, Coalson JJ, Giavedoni LD, Anzueto A, Orihuela CJ. A Non-Human Primate Model of Severe Pneumococcal Pneumonia. *PloS one* 2016; 11: e0166092.

29. Tettelin H, Nelson KE, Paulsen IT, Eisen JA, Read TD, Peterson S, Heidelberg J, DeBoy RT, Haft DH, Dodson RJ, Durkin AS, Gwinn M, Kolonay JF, Nelson WC, Peterson JD, Umayam LA, White O, Salzberg SL, Lewis MR, Radune D, Holtzapple E, Khouri H,

AJRCCM Articles in Press. Published on 14-June-2017 as 10.1164/rccm.201701-0104OC

Wolf AM, Utterback TR, Hansen CL, McDonald LA, Feldblyum TV, Angiuoli S, Dickinson T, Hickey EK, Holt IE, Loftus BJ, Yang F, Smith HO, Venter JC, Dougherty BA, Morrison DA, Hollingshead SK, Fraser CM. Complete genome sequence of a virulent isolate of Streptococcus pneumoniae. *Science* 2001; 293: 498-506.

30. Giavedoni LD. Simultaneous detection of multiple cytokines and chemokines from nonhuman primates using luminex technology. *J Immunol Methods* 2005; 301: 89-101.
31. Bujak M, Frangogiannis NG. The role of TGF-beta signaling in myocardial infarction and cardiac remodeling. *Cardiovasc Res* 2007; 74: 184-195.
32. Paizis G, Gilbert RE, Cooper ME, Murthi P, Schembri JM, Wu LL, Rumble JR, Kelly DJ, Tikellis C, Cox A, Smallwood RA, Angus PW. Effect of angiotensin II type 1 receptor blockade on experimental hepatic fibrogenesis. *Journal of hepatology* 2001; 35: 376-385.
33. Goldsmith EC, Bradshaw AD, Spinale FG. Cellular mechanisms of tissue fibrosis. 2. Contributory pathways leading to myocardial fibrosis: moving beyond collagen expression. *American journal of physiology Cell physiology* 2013; 304: C393-402.
34. Kim JH, Park MY, Kim CN, Kim KH, Kang HB, Kim KD, Kim JW. Expression of endothelial cell-specific molecule-1 regulated by hypoxia inducible factor-1alpha in human colon carcinoma: impact of ESM-1 on prognosis and its correlation with clinicopathological features. *Oncology reports* 2012; 28: 1701-1708.
35. Restrepo MI, Mortensen EM, Rello J, Brody J, Anzueto A. Late admission to the ICU in patients with community-acquired pneumonia is associated with higher mortality. *Chest* 2010; 137: 552-557.
36. Mandell LA, Wunderink RG, Anzueto A, Bartlett JG, Campbell GD, Dean NC, Dowell SF, File TM, Jr., Musher DM, Niederman MS, Torres A, Whitney CG, Infectious Diseases

Society of A, American Thoracic S. Infectious Diseases Society of America/American Thoracic Society consensus guidelines on the management of community-acquired pneumonia in adults. *Clinical infectious diseases : an official publication of the Infectious Diseases Society of America* 2007; 44 Suppl 2: S27-72.

37. Rudiger A, Singer M. The heart in sepsis: from basic mechanisms to clinical management. *Curr Vasc Pharmacol* 2013; 11: 187-195.

38. Zaky A, Gill EA, Lin CP, Paul CP, Bendjelid K, Treggiari MM. Characteristics of sepsis-induced cardiac dysfunction using speckle-tracking echocardiography: a feasibility study. *Anaesth Intensive Care* 2016; 44: 65-76.

39. Ammann P, Fehr T, Minder EI, Gunter C, Bertel O. Elevation of troponin I in sepsis and septic shock. *Intensive care medicine* 2001; 27: 965-969.

40. Altmann DR, Korte W, Maeder MT, Fehr T, Haager P, Rickli H, Kleger GR, Rodriguez R, Ammann P. Elevated cardiac troponin I in sepsis and septic shock: no evidence for thrombus associated myocardial necrosis. *PloS one* 2010; 5: e9017.

41. Vestjens SM, Spoorenberg SM, Rijkers GT, Grutters JC, Ten Berg JM, Noordzij PG, Van de Garde EM, Bos WJ, Ovidius Study G. High-sensitivity cardiac troponin T predicts mortality after hospitalization for community-acquired pneumonia. *Respirology* 2017.

42. Chiong M, Wang ZV, Pedrozo Z, Cao DJ, Troncoso R, Ibacache M, Criollo A, Nemchenko A, Hill JA, Lavandero S. Cardiomyocyte death: mechanisms and translational implications. *Cell Death Dis* 2011; 2: e244.

43. Lee P, Sata M, Lefer DJ, Factor SM, Walsh K, Kitsis RN. Fas pathway is a critical mediator of cardiac myocyte death and MI during ischemia-reperfusion in vivo. *Am J Physiol Heart Circ Physiol* 2003; 284: H456-463.

AJRCCM Articles in Press. Published on 14-June-2017 as 10.1164/rccm.201701-0104OC

44. Pasparakis M, Vandenabeele P. Necroptosis and its role in inflammation. *Nature* 2015; 517: 311-320.

45. Silke J, Rickard JA, Gerlic M. The diverse role of RIP kinases in necroptosis and inflammation. *Nature immunology* 2015; 16: 689-697.

46. Yin B, Xu Y, Wei RL, He F, Luo BY, Wang JY. Inhibition of receptor-interacting protein 3 upregulation and nuclear translocation involved in Necrostatin-1 protection against hippocampal neuronal programmed necrosis induced by ischemia/reperfusion injury. *Brain Res* 2015; 1609: 63-71.

47. Souders CA, Bowers SL, Baudino TA. Cardiac fibroblast: the renaissance cell. *Circulation research* 2009; 105: 1164-1176.

48. Mann DL. Inflammatory mediators and the failing heart: past, present, and the foreseeable future. *Circulation research* 2002; 91: 988-998.

49. Aliberti S, Ramirez JA. Cardiac diseases complicating community-acquired pneumonia. *Current opinion in infectious diseases* 2014; 27: 295-301.

50. Amsterdam EA, Wenger NK, Brindis RG, Casey DE, Jr., Ganiats TG, Holmes DR, Jr., Jaffe AS, Jneid H, Kelly RF, Kontos MC, Levine GN, Liebson PR, Mukherjee D, Peterson ED, Sabatine MS, Smalling RW, Zieman SJ, American College of C, American Heart Association Task Force on Practice G, Society for Cardiovascular A, Interventions, Society of Thoracic S, American Association for Clinical C. 2014 AHA/ACC Guideline for the Management of Patients with Non-ST-Elevation Acute Coronary Syndromes: a report of the American College of Cardiology/American Heart Association Task Force on Practice Guidelines. *J Am Coll Cardiol* 2014; 64: e139-228.

FIGURE LEGENDS

Figure 1. Non-human primates with severe pneumococcal pneumonia developed diffuse nonspecific repolarization abnormalities. 12-lead Electrocardiograms (ECGs) were recorded at baseline (A) and at the end of the experiment (B-E). At baseline, all animals were in sinus rhythm with no repolarization abnormalities (A). After development of pneumococcal pneumonia, the ECGs consistently showed sinus tachycardia (B, C), and abnormal repolarization (i.e., diffuse T wave and ST segment flattering) (B, C, D, E).

Figure 2. Serum concentrations of cardiac damage biomarkers were elevated in animals with acute and convalescent pneumococcal pneumonia. The serum biomarkers of cardiac damage, Troponin T, heart fatty acid binding protein (H-FABP) and N-terminal pro-brain natriuretic peptide (NT-proBNP), were assessed pre-infection, at days 4-6 for acute group and at days 9-14 for convalescent group. Median (n=6) serum concentration of Troponin T (A), H-FABP (B) and NT-proBNP (C) are shown pre-infection and at the end of the experiment (i.e., before euthanasia). To test whether antibiotic treatment could prevent cardiac damage, the cohort was stratified into NHP with acute pneumonia (i.e., without antibiotics, n=6) and those convalescent pneumonia (i.e., with antibiotics, n=3). Serum levels of Troponin T (B), H-FABP (D) and NT-proBNP (F) were assessed for each group pre-infection, at days 4-6 for acute group and at days 9-14 for convalescent group. Values are shown as medians with interquartile ranges (IQR). The paired non-parametric Wilcoxon signed rank test was used to analyze statistical differences among the groups. *, $p< 0.05$; ** $p< 0.01$; ** $p< 0.001$; n.s., not significant.

AJRCCM Articles in Press. Published on 14-June-2017 as 10.1164/rccm.201701-0104OC

Figure 3. *Streptococcus pneumoniae* translocates into the heart during pneumonia. Representative images from left ventricular (A, C) and interventricular septal (B) sections from the 6 NHP with pneumococcal pneumonia and 3 uninfected controls (D). *S. pneumoniae* were visualized using immunofluorescence staining with antiserum against serotype 4 capsular polysaccharide (CPS) (green) and DAPI to reveal nucleated tissue cells. Bacterial aggregates with diplococci morphology are seen within the left ventricles and septa of NHP with acute pneumonia (A, B). Bacterial cluster conformation indicates active replication (A). Single capsule debris were scattered throughout the left ventricles and in the interventricular septa of convalescent NHP (C). Pneumococcal capsules were not identified in the hearts of uninfected control NHP (D).

Figure 4. Hearts of Non-human primates (NHP) with severe pneumonia developed severe cardiac injury with variable pathological characteristics. Representative hematoxylin & eosin (H&E) and transmission electron microscopy (TEM) images of heart specimens from NHP with acute pneumococcal pneumonia (A, B, E) and convalescent pneumonia (C, F, G), and uninfected control NHP (D, H). NHP developed myocyte cytoplasm degenerative changes including fatty change, vacuolization, and myofibrillar separation (A, G). Perinuclear and interstitial edema are evident, and several myocyte nuclei contain condensed chromation, a necrotic change (A, E). Additionally, in the left ventricle myocytes with cytoplasmic changes of contraction bands, focal vacuolization, and myocytolysis were identified (B, F). The edematous interstitium contained increased small mononuclear cells and some neutrophiles (B). Nuclear edema and karyolyis are diffusely evident in cardiomyocytes (B, G). Widespread myocytolysis, contraction bands,

striking nuclear pyknosis, and karyolysis are seen in the septum (C, E, F). Finally, mitochondrial cristae degradation and edema were consistently observed by TEM (F, G).

Figure 5. Cytokines and chemokines present in homogenized heart of non-human primates (NHP) with acute and convalescent pneumococcal pneumonia. Median concentrations of pro-inflammatory cytokines in homogenized left ventricles and interventricular septa of NHP with acute and convalescent pneumococcal pneumonia. NHP with acute pneumonia had higher concentrations of interleukin (IL)-6 (A), tumor necrosis factor (TNF)-α (B), IL-8 (C), IL-1β, IL-1Rα (E), and macrophage inflammatory protein (MIP)-1α compared to uninfected NHP. Convalescent NHP had lower concentrations of cytokines than NHP with acute pneumonia, but IL-6(A), TNFα (B), IL-8 (C), and IL-1β (E) persisted at higher levels than uninfected controls. Values are shown as medians and interquartile ranges (IQR). The unpaired nonparametric Mann-Whitney U test was used to analyze statistical differences among the groups. All comparisons were made against uninfected controls. *, $p< 0.05$; ** $p< 0.01$; ** $p< 0.001$; n.s., not significant.

Figure 6. Necroptosis in heart tissue increases after antibiotic treatment.
Immunohistochemistry (IHC) was used to elucidate the cell pathways involved during cell death in NHP with pneumococcal pneumonia. IHC of heart sections stained for receptor-interacting protein kinase 3 (RIP3) and phosphorylated mixed lineage kinase domain like pseudokinase (pMLKL) (A-B). (C) Immunoblot for RIP3, pMLKL, and SDHA (loading control) in heart tissue of infected NHP vs uninfected control. (D) Relative levels of RIP3 and pMLKL protein expression determined by comparing the ratio of the detected band versus total protein levels as

AJRCCM Articles in Press. Published on 14-June-2017 as 10.1164/rccm.201701-0104OC

determined using LI-COR Image Studio Lite. Values are shown as medians and interquartile ranges (IQR). The unpaired nonparametric Mann-Whitney U tests was used to analyze statistical differences among the groups. *, $P < 0.05$; n.s., not significant.

Figure 7: *S. pneumoniae* induces *de novo* collagen deposition in non-human primates (NHP) with convalescent pneumonia. Representative images of heart sections from the six NHP infected with *S. pneumoniae* and three uninfected controls. Picosirus red was used to identify collagen deposition (A). NHP with convalescent pneumonia developed collagen deposition throughout the left ventricle and interventricular septum (A). Transmission electron microscopy (TEM) was used to confirm collagen deposition (B), identifying areas with conglomerates of collagen fibers in NHP that survived the acute pneumonia (B). The upregulation of pSMAD3 in convalescent NHP was identified by immunoblots (C) and relative protein levels (pSMAD3/SDHA [loading control]) (D) were determined using LI-COR Image Studio Lite. Values are shown as medians and interquartile ranges (IQR). The unpaired nonparametric Mann-Whitney U tests was used to analyze statistical differences among the groups. *, $P < 0.05$; n.s., not significant.

TABLES

Table 1. Twelve lead electrocardiogram quantitative analysis of all 6 non-human primates.

Variable	Baseline	End of Experiment	p value
Heart rate, bpm	78 (69, 99.5)	122 (102.5, 152)	**0.001**
P wave duration, ms	80 (76.5, 87.5)	80 (70, 100)	0.728
PR interval, ms	140 (121.5, 155)	135 (125, 155)	0.893
RR interval, ms	769.23 (603.15, 869.74)	491.93 (394.73, 586.36)	**0.001**
QRS interval, ms	55 (47.5, 62.5)	55 (50, 63.75)	0.874
QT interval, ms	310 (287.5, 347.5)	292.50 (281.25, 317.5)	0.323
Corrected QT, ms	369.76 (341.53, 398.36)	440.20 (398.29, 454.36)	**0.001**
ST segment, ms	125 (100, 160)	114 (91.25, 132.5)	0.308
T wave, ms	125 (120, 140)	130 (125, 143.75)	0.229

Table 2. Qualitative individual interpretation of 12-lead ECG's at baseline and the end of the experiment.

		Electrocardiographic Findings	
	Animal	**Baseline**	**End of Experiment**
Acute pneumonia	1	Biphasic T waves in lateral leads	Inverted T waves inferior and anterolateral leads
	2	No repolarization abnormalities	Slow ventricular rhythm
	3	Diffuse ST and T wave flattening	Q waves on lateral leads, ST segment and T wave flattening in inferolateral leads
Convalescent pneumonia	4	No repolarization abnormalities	Diffuse ST segment and T wave flattening
	5	Short QT segment	Diffuse ST segment and T wave flattening
	6	No repolarization abnormalities	Q waves on lateral leads, T wave inversion lateral leads and ST segment depression inferior leads

AJRCCM Articles in Press. Published on 14-June-2017 as 10.1164/rccm.201701-0104OC

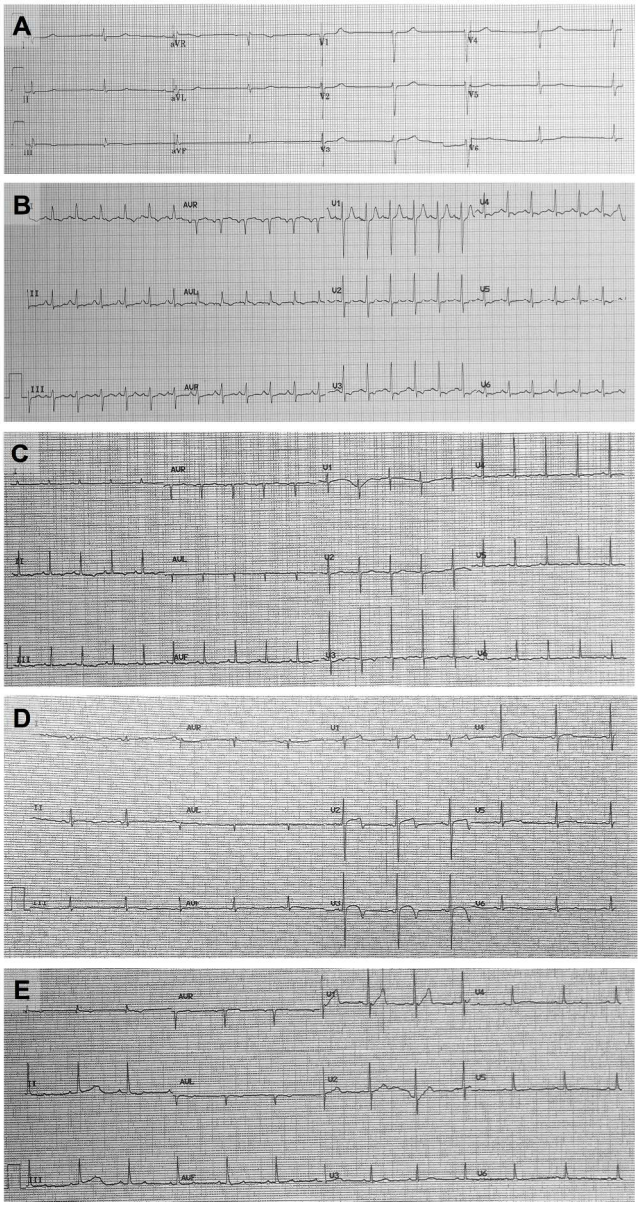

Figure 1. Non-human primates with severe pneumococcal pneumonia developed diffuse nonspecific repolarization abnormalities. 12-lead Electrocardiograms (ECGs) were recorded at baseline (A) and at the end of the experiment (B-E). At baseline, all animals were in sinus rhythm with no repolarization abnormalities (A). After development of pneumococcal pneumonia, the ECGs consistently showed sinus tachycardia (B, C), and abnormal repolarization (i.e., diffuse T wave and ST segment flattering) (B, C, D, E).

157x294mm (300 x 300 DPI)

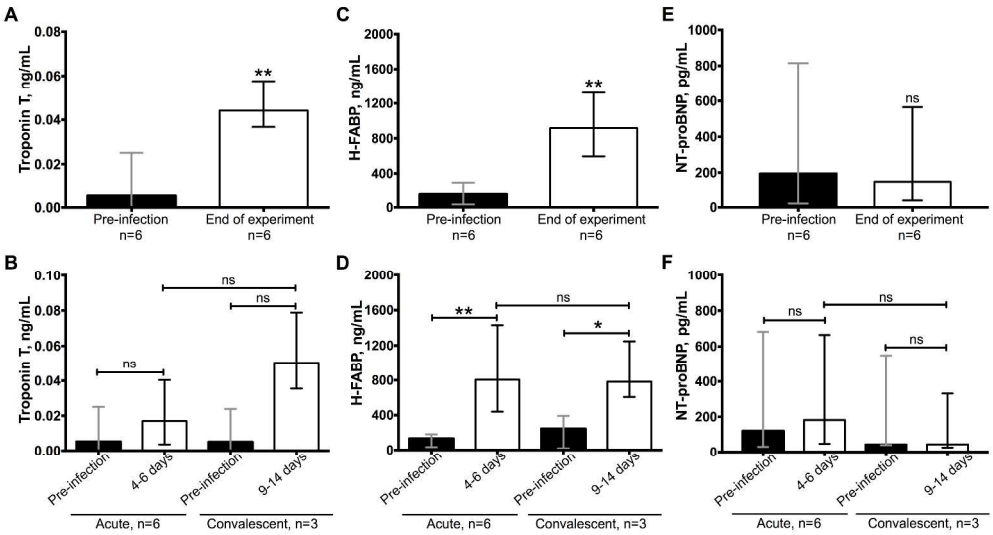

Figure 2. Serum concentrations of cardiac damage biomarkers were elevated in animals with acute and convalescent pneumococcal pneumonia. The serum biomarkers of cardiac damage, Troponin T, heart fatty acid binding protein (H-FABP) and N-terminal pro-brain natriuretic peptide (NT-proBNP), were assessed pre-infection, at days 4-6 for acute group and at days 9-14 for convalescent group. Median (n=6) serum concentration of Troponin T (A), H-FABP (B) and NT-proBNP (C) are shown pre-infection and at the end of the experiment (i.e., before euthanasia). To test whether antibiotic treatment could prevent cardiac damage, the cohort was stratified into NHP with acute pneumonia (i.e., without antibiotics, n=6) and those convalescent pneumonia (i.e., with antibiotics, n=3). Serum levels of Troponin T (B), H-FABP (D) and NT-proBNP (F) were assessed for each group pre-infection, at days 4-6 for acute group and at days 9-14 for convalescent group. Values are shown as medians with interquartile ranges (IQR). The paired non-parametric Wilcoxon signed rank test was used to analyze statistical differences among the groups. *, p< 0.05; ** p< 0.01; ** p< 0.001; n.s., not significant.

476x262mm (300 x 300 DPI)

AJRCCM Articles in Press. Published on 14-June-2017 as 10.1164/rccm.201701-0104OC

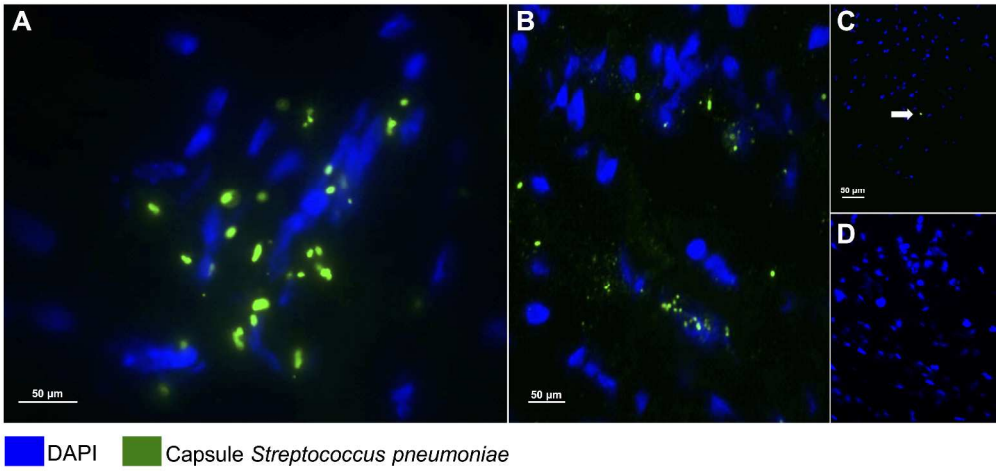

Figure 3. Streptococcus pneumoniae translocates into the heart during pneumonia. Representative images from left ventricular (A, C) and interventricular septal (B) sections from the 6 NHP with pneumococcal pneumonia and 3 uninfected controls (D). S. pneumoniae were visualized using immunofluorescence staining with antiserum against serotype 4 capsular polysaccharide (CPS) (green) and DAPI to reveal nucleated tissue cells. Bacterial aggregates with diplococci morphology are seen within the left ventricles and septa of NHP with acute pneumonia (A, B). Bacterial cluster conformation indicates active replication (A). Single capsule debris were scattered throughout the left ventricles and in the interventricular septa of convalescent NHP (C). Pneumococcal capsules were not identified in the hearts of uninfected control NHP (D).

658x317mm (300 x 300 DPI)

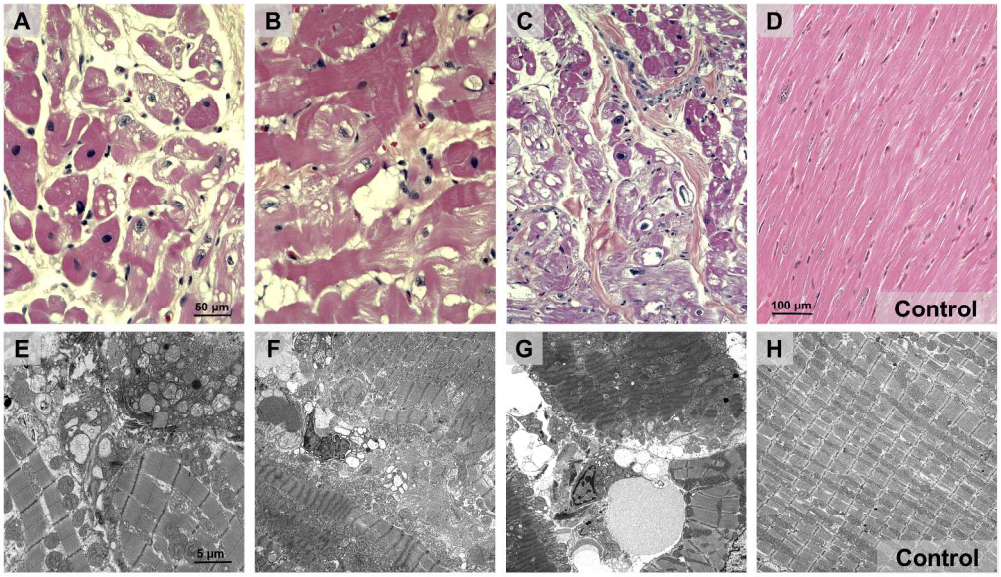

Figure 4. Hearts of Non-human primates (NHP) with severe pneumonia developed severe cardiac injury with variable pathological characteristics. Representative hematoxylin & eosin (H&E) and transmission electron microscopy (TEM) images of heart specimens from NHP with acute pneumococcal pneumonia (A, B, E) and convalescent pneumonia (C, F, G), and uninfected control NHP (D, H). NHP developed myocyte cytoplasm degenerative changes including fatty change, vacuolization, and myofibrillar separation (A, G). Perinuclear and interstitial edema are evident, and several myocyte nuclei contain condensed chromation, a necrotic change (A, E). Additionally, in the left ventricle myocytes with cytoplasmic changes of contraction bands, focal vacuolization, and myocytolysis were identified (B, F). The edematous interstitium contained increased small mononuclear cells and some neutrophiles (B). Nuclear edema and karyolyis are diffusely evident in cardiomyocytes (B, G). Widespread myocytolysis, contraction bands, striking nuclear pyknosis, and karyolysis are seen in the septum (C, E, F). Finally, mitochondrial cristae degradation and edema were consistently observed by TEM (F, G).

595x368mm (300 x 300 DPI)

AJRCCM Articles in Press. Published on 14-June-2017 as 10.1164/rccm.201701-0104OC

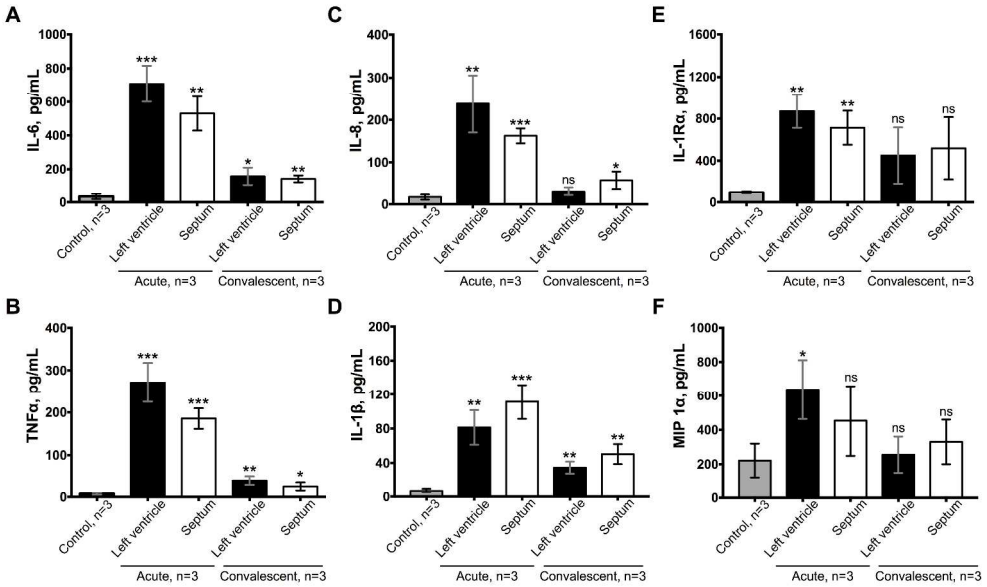

Figure 5. Cytokines and chemokines present in homogenized heart of non-human primates (NHP) with acute and convalescent pneumococcal pneumonia. Median concentrations of pro-inflammatory cytokines in homogenized left ventricles and interventricular septa of NHP with acute and convalescent pneumococcal pneumonia. NHP with acute pneumonia had higher concentrations of interleukin (IL)-6 (A), tumor necrosis factor (TNF)-α (B), IL-8 (C), IL-1β, IL-1Rα (E), and macrophage inflammatory protein (MIP)-1α compared to uninfected NHP. Convalescent NHP had lower concentrations of cytokines than NHP with acute pneumonia, but IL-6(A), TNFα (B), IL-8 (C), and IL-1β (E) persisted at higher levels than uninfected controls. Values are shown as medians and interquartile ranges (IQR). The unpaired nonparametric Mann-Whitney U test was used to analyze statistical differences among the groups. All comparisons were made against uninfected controls. *, p< 0.05; ** p< 0.01; ** p< 0.001; n.s., not significant.

497x296mm (300 x 300 DPI)

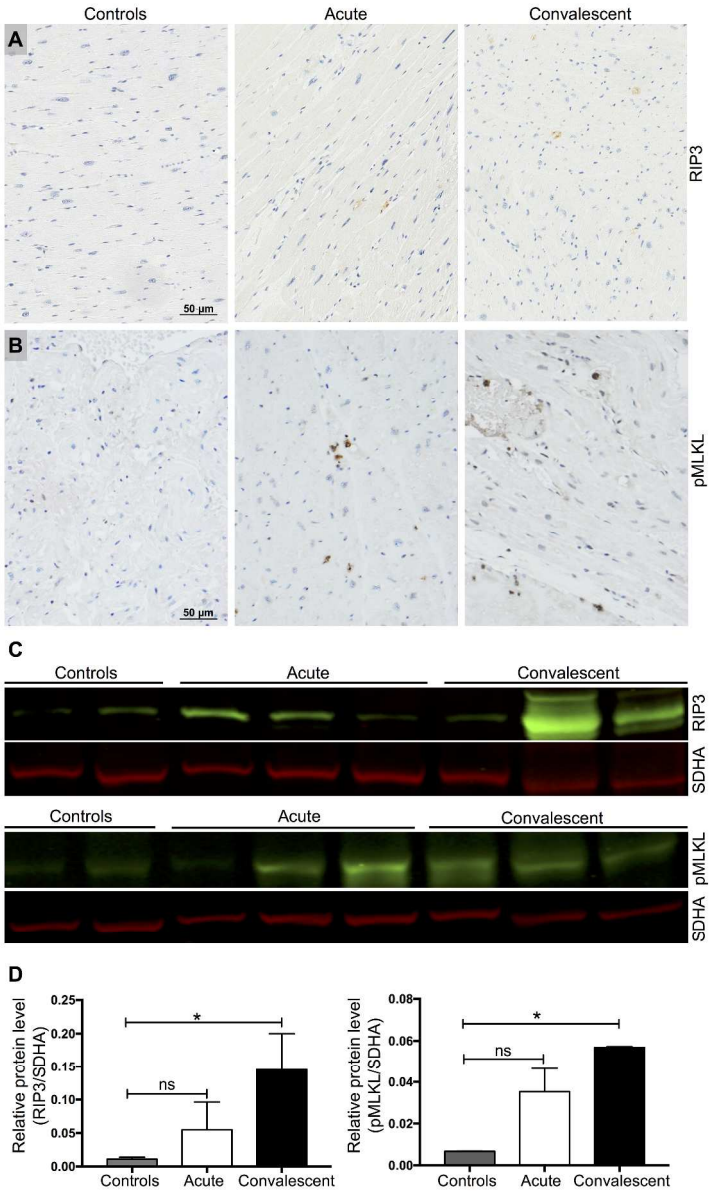

Figure 6. Necroptosis in heart tissue increases after antibiotic treatment. Immunohistochemistry (IHC) was used to elucidate the cell pathways involved during cell death in NHP with pneumococcal pneumonia. IHC of heart sections stained for receptor-interacting protein kinase 3 (RIP3) and phosphorylated mixed lineage kinase domain like pseudokinase (pMLKL) (A-B). (C) Immunoblot for RIP3, pMLKL, and SDHA (loading control) in heart tissue of infected NHP vs uninfected control. (D) Relative levels of RIP3 and pMLKL protein expression determined by comparing the ratio of the detected band versus total protein levels as determined using LI-COR Image Studio Lite. Values are shown as medians and interquartile ranges (IQR). The unpaired nonparametric Mann-Whitney U tests was used to analyze statistical differences among the groups. *, $P < 0.05$; n.s., not significant.

486x808mm (250 x 250 DPI)

AJRCCM Articles in Press. Published on 14-June-2017 as 10.1164/rccm.201701-0104OC

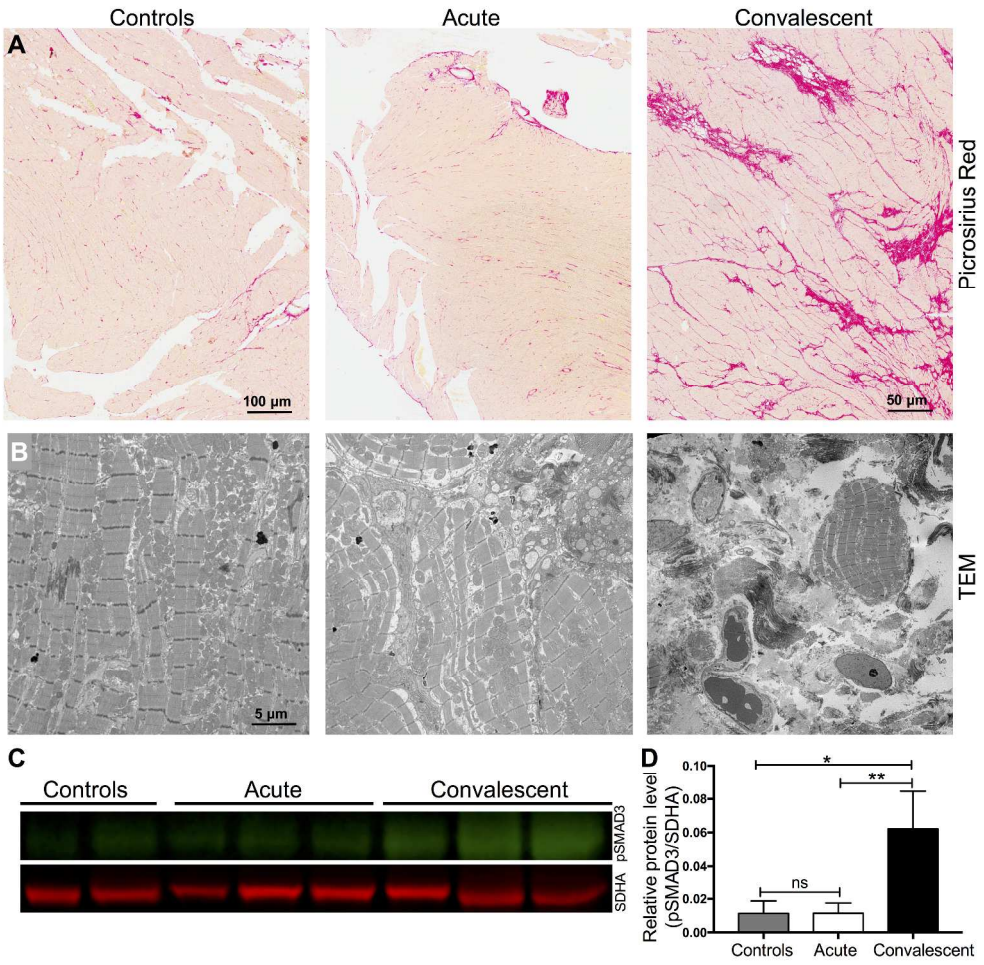

Figure 7: S. pneumoniae induces de novo collagen deposition in non-human primates (NHP) with convalescent pneumonia. Representative images of heart sections from the six NHP infected with S. pneumoniae and three uninfected controls. Picosirus red was used to identify collagen deposition (A). NHP with convalescent pneumonia developed collagen deposition throughout the left ventricle and interventricular septum (A). Transmission electron microscopy (TEM) was used to confirm collagen deposition (B), identifying areas with conglomerates of collagen fibers in NHP that survived the acute pneumonia (B). The upregulation of pSMAD3 in convalescent NHP was identified by immunoblots (C) and relative protein levels (pSMAD3/SDHA [loading control]) (D) were determined using LI-COR Image Studio Lite. Values are shown as medians and interquartile ranges (IQR). The unpaired nonparametric Mann-Whitney U tests was used to analyze statistical differences among the groups. *, $P < 0.05$; n.s., not significant.

499x484mm (300 x 300 DPI)

AJRCCM Articles in Press. Published on 14-June-2017 as 10.1164/rccm.201701-0104OC

ONLINE DATA SUPPLEMENT

TITLE: Severe Pneumococcal Pneumonia Causes Acute Cardiac Toxicity and Subsequent Cardiac Remodeling

AUTHORS: Luis F. Reyes[1, 2#], Marcos I. Restrepo[1, 2#], Cecilia A. Hinojosa[1, 2], Nilam J. Soni[1, 2], Antonio Anzueto[1,2], Bettina L. Babu[1, 2], Norberto Gonzalez-Juarbe[3], Alejandro H. Rodriguez[4], Alejandro Jimenez[5], James D. Chalmers[6], Stefano Aliberti[7], Oriol Sibila[8], Vicki T. Winter[9], Jacqueline J. Coalson[9], Luis D. Giavedoni[10], Charles S. Dela Cruz[11], Grant W. Waterer[12], Martin Witzenrath[13], Norbert Suttorp[13], Peter H. Dube[14] and Carlos J. Orihuela[3].

SUPPLEMENTARY TABLES

Table A. Demographics and Clinical Characteristics of Non-Human Primates with confirmed pneumococcal pneumonia

Variables	Acute n= 3	Convalescent n= 3	p value
Age, years, mean (SD)	12.3 (4.0)	17.3 (5.6)	0.28
Male, n (%)	3 (100)	1 (33)	0.41
Systemic inflammatory response (SIRS) parameters, mean (SD)			
Heart rate, beats/min	144.7 (8.3)	139.3 (7.6)	0.45
Temperature, ^{o}C	102.7 (1.5)	102.3 (1.5)	0.80
White blood cells, thousands/mm^3	5.7 (2.1)	4.9 (1.2)	0.58
Bands, %	4.0 (4.3)	2 (3.4)	0.56
Bacteremia, Log_{10} (CFU/ml)	3.9 (0.7)	4.6 (0.7)	0.27
Pneumonia severity, mean (SD)			

AJRCCM Articles in Press. Published on 14-June-2017 as 10.1164/rccm.201701-0104OC

Neutrophils, %	66.6 (13.3)	87 (2.0)	0.06
Lymphocytes, thousands/mm^3	1.3 (0.3)	0.9 (0.4)	0.23
Hemoglobin, gr/dL	11.7 (0.8)	10.5 (0.7)	0.15
Platelets, thousands/mm^3	242.3 (52.5)	264.3 (27.5)	0.55
Creatinine, md/dL	0.7 (0.1)	0.7 (0.2)	0.99
Blood urea nitrogen, mg/dL	7.6 (2.8)	12.3 (4.9)	0.23
Glucose, md/dL	88.6 (9.5)	110.0 (20.3)	0.17
Aspartate transaminase, U/L	41.0 (12.7)	36.0 (12.7)	0.65
Alkaline phosphatase, U/L	447.7 (214.2)	336.3 (40.6)	0.42
Albumin, gr/dL	2.7 (0.2)	2.7 (0.1)	0.74
pH	7.5 (0.02)	7.5 (0.06)	0.61
Lactate, mM/L	1.8 (0.2)	2.1 (0.2)	0.16

Table B. 12 lead electrocardiograms characteristics in all the baboons.

	Baseline				**End of the experiment**		
Variable	**Acute**	**Convalescent**	**p value**		**Acute**	**Convalescent**	**p value**
Heart rate, bpm	95 ± 18.9	75.1 ± 9.2	**0.01**		134.8 ±22.2	104.7 ± 45.	0.08
P wave duration, ms	82.2 ± 6.7	77.5 ± 17.6	0.40		93.8 ±25.1	79.1 ± 15.1	0.14
PR interval, ms	139.2 ± 12.2	136.7 ± 25.3	0.76		137.2 ±13.9	126.5 ± 47.9	0.51
R-R interval, ms	654.3 ± 160.2	808.2 ± 89.3	**0.01**		456.4 ±80.3	848.4 ±856.4	0.19
R-R interval, sec	0.6 ± 0.2	0.8 ± 0.1	**0.01**		0.5 ± 0.1	0.8 ± 0.9	0.19
QRS interval, ms	47.2 ± 7.9	62.8± 12.2	**0.02**		51.1 ± 7.8	99.1 ±136.6	0.27
QT interval, ms	317.7 ±40.4	307 ± 63.6	0.64		283.7 ± 18.8	323.5 ± 41.4	**0.02**
Corrected QT, ms	395.1 ± 20.5	342.2 ±67.8	**0.02**		417.9 ± 37.6	440.8 ±73.1	0.44
ST segment, ms	139.4 ± 51.5	119.5 ± 51.0	0.39		101.2 ±17.2	129.7 ±23.2	**0.01**
T wave, ms	131.1 ±14.7	124.5 ±19.3	0.39		131.8 ±11.9	134.3 ±13.2	0.69
Bpm: beats per minute; sec: seconds; ms: milliseconds							

AJRCCM Articles in Press. Published on 14-June-2017 as 10.1164/rccm.201701-0104OC

Table C. Summary findings of the focused cardiac ultrasound (FCU) examination conducted at baseline and at the end of the experiment.

GROUP	BABOON	ORGAN	BASELINE	END OF THE EXPERIMENT
Acute pneumonia	1	Left Ventricular Function	Normal LVSF (50-55%)	Normal LVSF (50-55%)
		Right Ventricular Function	Normal RVSF	Normal RVSF
		Valves	Normal	Normal
		Pericardium	Normal	Normal
		IVC	Normal CVP (5mm Hg)	Low CVP (<5mm Hg)
	2	Left Ventricular Function	Normal LVSF	No images due to sudden death
		Right Ventricular Function	Normal RVSF	
		Valves	Normal	
		Pericardium	Normal	
		IVC	Normal	
	3	Left Ventricular Function	Normal LVSF (50-55%)	Hyperdynamic LVSF (65-70%)
		Right Ventricular Function	Normal RVSF	Normal RVSF
		Valves	Normal	Moderate tricuspid regurgitation
		Pericardium	Normal	Small pericardial effusion
		IVC	Normal	Collapsed (CVP <5) 0.60/0.25
		Comments		Lungs of this animal had severe pneumonia
	4	Left Ventricular Function	Normal LVSF (50-55%)	Normal LVSF (50-55%)
		Right Ventricular Function	Normal RVSF	Normal LVSF & RVSF, NL RV and LV size, No WMAs
		Valves	Normal	Moderate TR
		Pericardium	Normal	Normal
		IVC	Normal	Collapsed (CVP <5)
		Comments		Bilateral hydronephrosis. RLL pneumonia looks better than Baboon #4 prior to euthanasia, but probably similar to baboon #3 (moderate severity). No

AJRCCM Articles in Press. Published on 14-June-2017 as 10.1164/rccm.201701-0104OC

				pleural effusions.
Convalescent pneumonia	5	Left Ventricular Function	Normal LVSF (50-55%)	Normal LVSF (50-55%), Significantly increase circumferential LV relative wall thickness (greater in inferior wall), mild inferior wall hypokinesis,
		Right Ventricular Function	Normal RVSF	Reduced RVSF, increased RV relative wall thickness, paradoxical septal motion
		Valves	Normal	Possible anterior mitral valve leaflet vegetation
		Pericardium	Normal	Small, complex pericardial effusion with septations
		IVC	Normal	Dilated, non-collapsible (CVP>15)
		Comments		Overall this was the sickest of the baboons that we have imaged.
	6	Left Ventricular Function	Normal LVSF (50-55%)	Normal LVSF (50-55%), Mild dilation of LV chamber, Significant increased circumferential LV relative wall thickness, no wall motion abnormalities
		Right Ventricular Function	Normal RVSF	Reduced RVSF, moderate RV chamber dilation, increased RV relative wall thickness
		Valves	Normal	Normal
		Pericardium	Normal	No pericardial effusion
		IVC	Collapsed (CVP <5)	Collapsed (CVP <5)
		Comments		Large left lower back abscess (vs. hematoma) around site of insertion of monitoring leads.

AJRCCM Articles in Press. Published on 14-June-2017 as 10.1164/rccm.201701-0104OC

SUPPLEMENTARY FIGURE LEGENDS

Figure A. Study design. Methods used for the non-invasively assessment of Major Cardiovascular Event (MACE) and invasive assessment of cardiac injury.

Figure B. Heart bacterial load. *S. pneumoniae* invades and replicates within the heart of NHP with acute severe pneumococcal pneumonia (i.e., without antibiotic treatment).

Figure C. ***S. pneumoniae*** **induces cardiac injury with different sizes and characteristics.** The variability in the size of the focal myocardial lesions that localize in perivascular sites is seen (A and B). The enlarged eosinophilic-stained myocytes in the lesions are sharply separated from surrounding myocardial tissue (A and B). H&E, 4x and 10x magnification, respectively.

Figure D. Cardiomyocytes died by apoptosis and necroptosis. CardioTAC staining was used to explore the presence of apoptosis in heart of NHP with severe pneumococcal pneumonia (A). Immunoblot for cleaved Caspase 3 and Actin (loading control) in heart tissue of infected NHP vs uninfected controls confirmed activation of apoptosis.

Figure E. Ischemia was not detected in the heart of NHP with severe pneumonia. Hypoxia was not detected using immunoblot for hypoxia inducible factor 1 (HIF1)-α and SDHA (loading control) in the heart of NHP with severe pneumococcal pneumonia independent of antibiotic treatment (acute vs. convalescent pneumonia).

AJRCCM Articles in Press. Published on 14-June-2017 as 10.1164/rccm.201701-0104OC

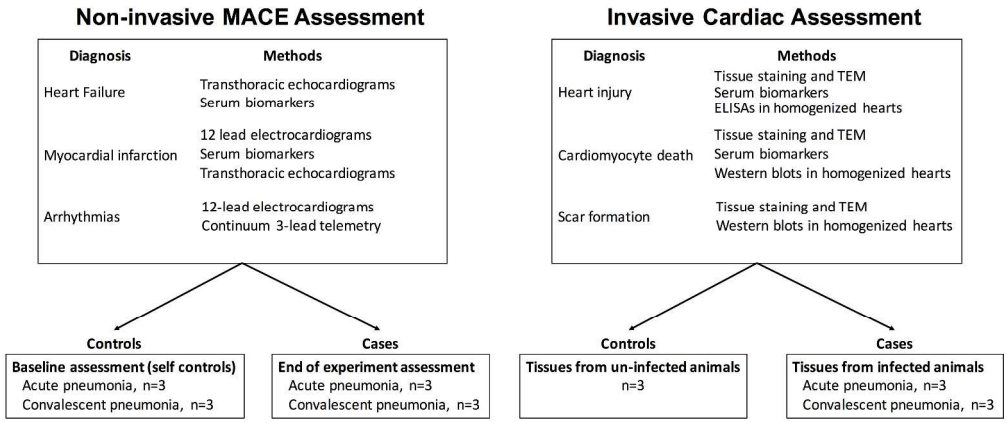

Figure A. Study design. Methods used for the non-invasively assessment of Major Cardiovascular Event (MACE) and invasive assessment of cardiac injury.

407x173mm (300 x 300 DPI)

AJRCCM Articles in Press. Published on 14-June-2017 as 10.1164/rccm.201701-0104OC

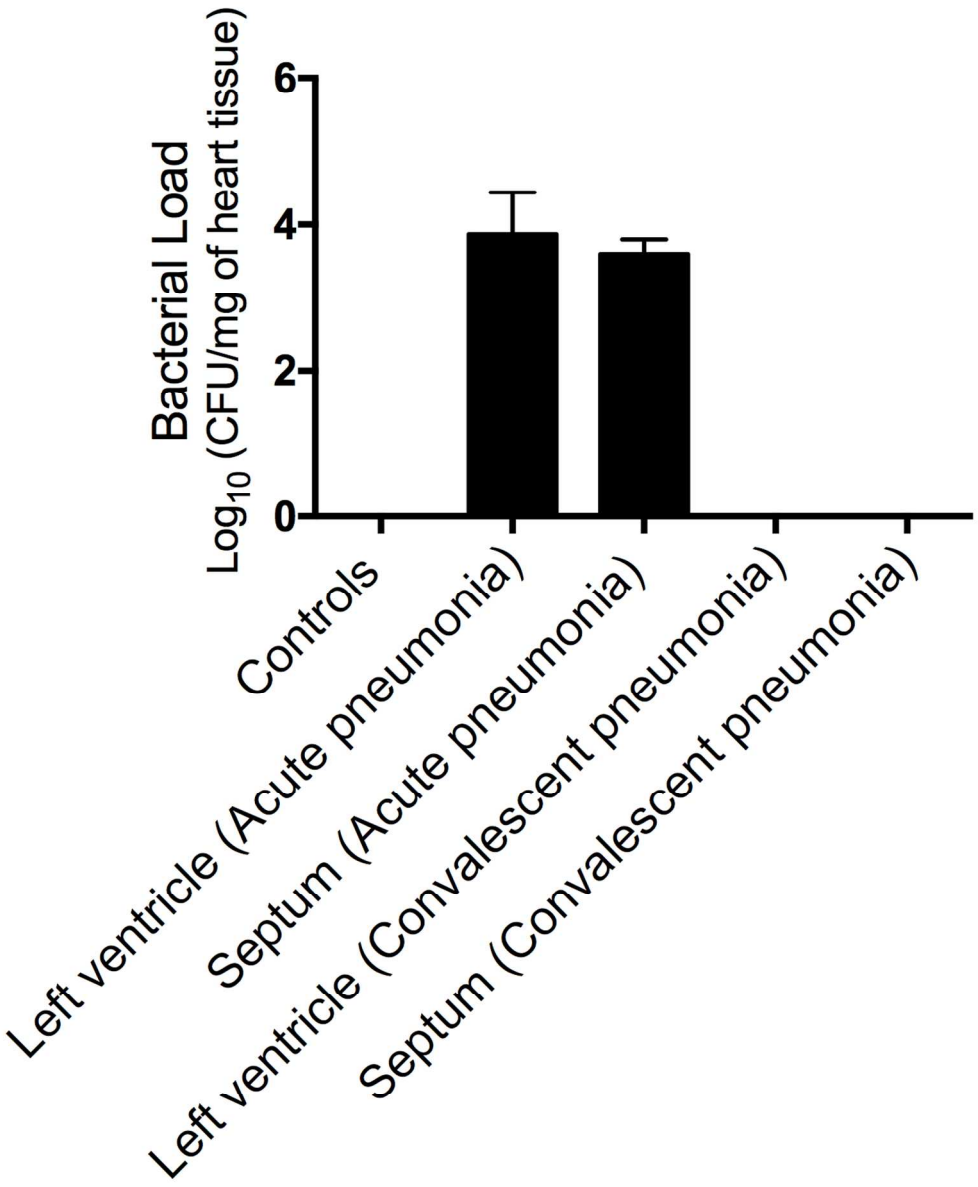

Figure B. Heart bacterial load. S. pneumoniae invades and replicates within the heart of NHP with acute severe pneumococcal pneumonia (i.e., without antibiotic treatment).

114x138mm (300 x 300 DPI)

AJRCCM Articles in Press. Published on 14-June-2017 as 10.1164/rccm.201701-0104OC

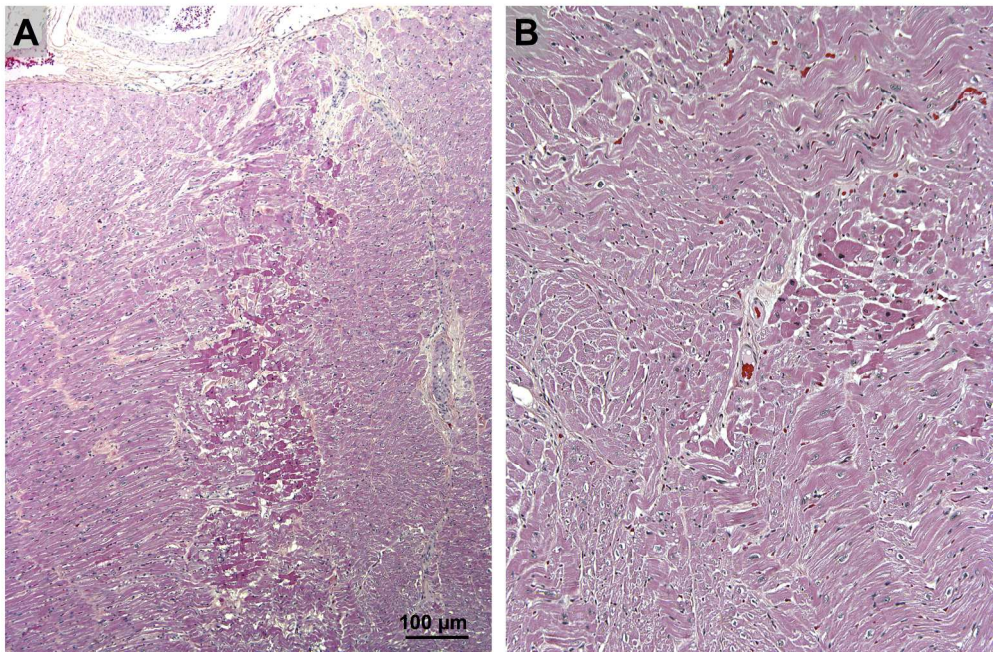

Figure C. S. pneumoniae induces cardiac injury with different sizes and characteristics. The variability in the size of the focal myocardial lesions that localize in perivascular sites is seen (A and B). The enlarged eosinophilic-stained myocytes in the lesions are sharply separated from surrounding myocardial tissue (A and B). H&E, 4x and 10x magnification, respectively.

354x231mm (250 x 250 DPI)

AJRCCM Articles in Press. Published on 14-June-2017 as 10.1164/rccm.201701-0104OC

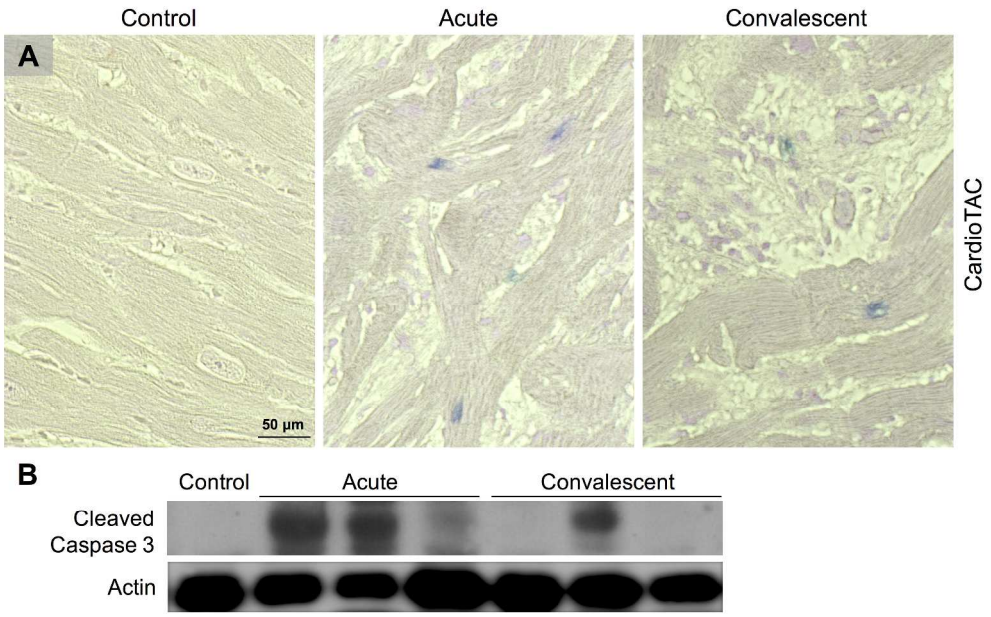

Figure D. Cardiomyocytes died by apoptosis and necroptosis. CardioTAC staining was used to explore the presence of apoptosis in heart of NHP with severe pneumococcal pneumonia (A). Immunoblot for cleaved Caspase 3 and Actin (loading control) in heart tissue of infected NHP vs uninfected controls confirmed activation of apoptosis.

485x299mm (250 x 250 DPI)

AJRCCM Articles in Press. Published on 14-June-2017 as 10.1164/rccm.201701-0104OC

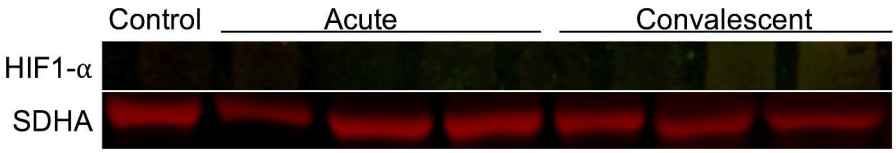

Figure E. Ischemia was not detected in the heart of NHP with severe pneumonia. Hypoxia was not detected using immunoblot for hypoxia inducible factor 1 (HIF1)-α and SDHA (loading control) in the heart of NHP with severe pneumococcal pneumonia independent of antibiotic treatment (acute vs. convalescent pneumonia).

367x59mm (300 x 300 DPI)